J Digit Imaging (2013) 26:797–802
DOI 10.1007/s10278-012-9547-6

Combination of Radiological and Gray Level Co-occurrence Matrix Textural Features Used to Distinguish Solitary Pulmonary Nodules by Computed Tomography

Haifeng Wu · Tao Sun · Jingjing Wang · Xia Li · Wei Wang · Da Huo · Pingxin Lv · Wen He · Keyang Wang · Xiuhua Guo

Published online: 17 January 2013

Abstract The objective of this study was to investigate the method of the combination of radiological and textural features for the differentiation of malignant from benign solitary pulmonary nodules by computed tomography. Features including 13 gray level co-occurrence matrix textural features and 12 radiological features were extracted from 2,117 CT slices, which came from 202 (116 malignant and 86 benign) patients. Lasso-type regularization to a nonlinear regression model was applied to select predictive features and a BP artificial neural network was used to build the diagnostic model. Eight radiological and two textural features were obtained after the Lasso-type regularization procedure. Twelve radiological features alone could reach an area under the ROC curve (AUC) of 0.84 in differentiating between malignant and benign lesions. The 10 selected characters improved the AUC to 0.91. The evaluation results showed that the method of selecting radiological and textural features appears to yield more effective in the distinction of malignant from benign solitary pulmonary nodules by computed tomography.

Keywords Radiological features · Textural features · Feature selection · Solitary pulmonary nodules · BP neural network

Haifeng Wu and Tao Sun contributed equally to this work

H. Wu · T. Sun · J. Wang · X. Li · W. Wang · D. Huo
School of Public Health and Family Medicine,
Capital Medical University,
Beijing 100069, China

X. Li · X. Guo (✉)
Beijing Municipal Key Laboratory of Clinical Epidemiology,
Beijing 100069, China
e-mail: guoxiuh@ccmu.edu.cn

P. Lv
Department of Radiology, Beijing Chest Hospital,
Capital Medical University,
Beijing 101149, China

W. He · K. Wang
Department of Radiology, Friendship Hospital,
Capital Medical University,
Beijing 100053, China

X. Guo
Department of Epidemiology and Health Statistics, School
of Public Health and Family Medicine, Capital Medical University,
Beijing 100069, China

Introduction

Lung cancer is the most common cause of cancer-related deaths [1], with a 5-year overall survival rate of only 15 % [2]. It is critical to detect and diagnose solitary pulmonary nodules (SPNs), since they are relevant to the choice of treatment and the survival rate [3]. Many computer-aided methods (CAD) have been proposed for SPNs [4–9]. In the CAD system, texture is a popular descriptor in the analysis and interpretation of images [10]. The gray level co-occurrence matrix (GLCM) is the most widely used texture analysis method in biological imaging [11], due to its ability to capture the spatial dependence of gray level values within an image [12].

Evaluation of specific morphological features of a solitary pulmonary nodule with conventional imaging techniques can help differentiate benign from malignant nodules and obviate further costly assessment [13]. Morphological characteristics of malignant solitary pulmonary nodules have been reported in terms of size, density, margin, contour, calcification, and cavitations [13, 14]. A prediction model has been developed based on these morphological predictors [15, 16].

In another study, McCarville et al. [8] collected 81 pulmonary nodules, based on CT findings to differ benign and

malignant nature of pulmonary nodules in pediatric patients, whereas Wang et al. [17] used the gray level co-occurrence matrix and the multi-level model to predict pulmonary nodules. Lee et al. [18] used a two-step approach for feature selection classifier ensemble construction to facilitate the prediction of characteristics of pulmonary nodules. Zhu et al. [19] presented a method to find and select texture features of solitary pulmonary nodules (SPNs) detected by computed tomography (CT) and evaluate the performance of support vector machine (SVM)-based classifiers in differentiating benign from malignant SPNs. Li et al. [20] established a clinical prediction model to estimate the probability of malignancy of SPNs using the morphological parameters. However, few considerations about the combination of textural descriptors and these morphological parameters have been introduced for SPN in CT [18].

In this study, a total of 25 features including shape/edge and textural features were extracted and Lasso-type regularization was implemented to select discriminative features for SPN of malignancy and to develop a parsimonious model. Lasso (least absolute shrinkage and selection operator) is an attractive regularization method for high-dimensional regression. It has been proved successful in several fields, including image processing and machine learning [21–23]. A BP neural network (BP NN) was utilized as a classifier. ROC was used to evaluate and compare the discrimination.

Materials and Methods

Materials

This study was performed with ethics approval (Ethics Committee of Xuanwu Hospital, Capital Medical University, approval document no. [2011] 01).

A total of 2,117 region of interests (ROIs) were acquired from 202 patients, with 846 benign ROI from 86 patients (42 males and 44 females) and 1,271 malignant ROIs from 116 patients (62 males and 54 females). The details are presented in Table 1. The morphological features were accessed by eight radiologists, and conflicts in final interpretation of CT images were resolved by consensus discussion.

A total of 1,573 ROIs acquired from 152 patients were randomly selected from the 202 cases as training data, with 577 benign ROIs from 61 patients (31 males and 30 females) and 996 malignant ROIs from 91 patients (51 males and 40 females). Five hundred forty-four ROIs acquired from the remaining 50 patients were used as test data, with 269 benign ROIs (25 benign cases: 11 males and 14 females) and 275 ROIs (25 malignant cases: 11 males and 14 females) of malignant tumors.

Table 1 The description of data set

	Number of cases	ROIs
Benign cases		
Tuberculosis	29	297
Inflammatory pseudotumor	15	143
Hamartoma	21	199
Pulmonary interstitial edema	2	16
Sclerosing hemangioma	12	110
Clear cell tumor	1	4
Benign cases diagnosed by 2 year follow-up	6	77
Malignant cases		
Glandular cancer	96	1,006
Squamous carcinoma	18	235
Malignant carcinoid tumor	2	30

All of the solitary pulmonary nodules in the CT images were segmented manually to obtain a ROI, and the textural features were extracted ROI by ROI. ROC curves were developed using information of cases.

CT scanning was performed either on a 64-slice helical CT scanner (GE/Light speed ultra System CT99, USA) or on a single-slice helical CT scanner (Picker 2000, USA). All scans had a per-slice size resolution of 512×512. The final diagnosis of lung cancer was confirmed by an operation or biopsy. The benign nodules were determined either pathologically or after a 2-year minimum follow-up.

Twelve subjective radiological features of the pulmonary nodules were quantitatively recorded. These were diameter, lymph node status (positive/negative), density (homogeneous or not), solid (yes or no), ground-glass opacity (yes or no), margin (smooth or speculated), lobulation (present or absent), nodules with an area of air (present or absent), calcification (present or absent), cavitations (present or absent), pleural indentation (present or absent), and pleural effusion (present or absent).

Nodule Segmentation and Textural Features Extraction

In order to eliminate all background pixels to avoid mistaking the edge between the artificial background and the organ as a textural feature, each ROI was further cropped using a gray level threshold algorithm which is a popular tool for image segmentation [24, 25]. Two thousand one hundred seventeen ROIs were generated. Figure 1 shows an example of the segmentation of a CT scan by the gray level threshold algorithm.

Once the medical images were pre-processed, as shown in Fig. 1, 13 textural features defined by Haralick et al. [26, 27] were extracted based on GLCM. The matrices recorded

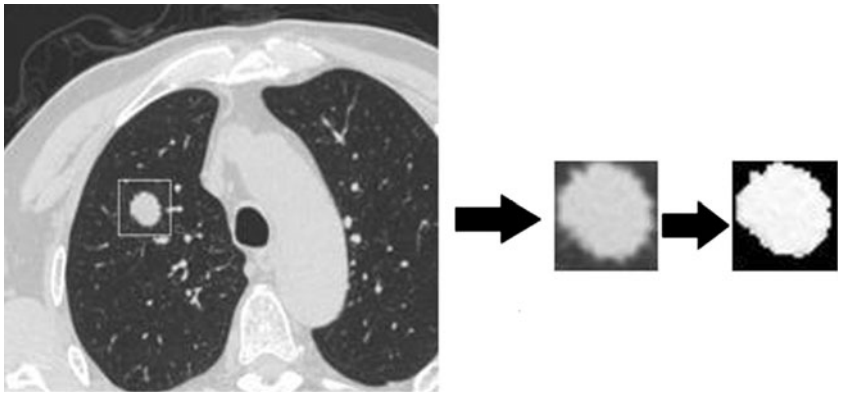

Fig. 1 Image segmentation using the gray level threshold algorithm

the frequencies at which a pair of points, separated by a specific distance and angle within a given region of interest, produced a specific pair of gray levels. The 13 commonly used textural descriptors (entropy, contrast, correlation, energy, homogeneity, inverse difference moment, variance, maximum probability, cluster tendency, sum-mean, difference-mean, sum-entropy, and difference-entropy) were calculated in this study.

Based on our previous study, we found that different parameters of GLCM have influence on the performance. Thus, a co-occurrence matrix was calculated for four directions (0°, 45° , 90° , 135°) at a distance of d=1. The feature values were then calculated as the mean values of the feature estimations for the four orientations. The image segmentation and textural features extraction were analyzed in MATLAB (version 7.3.0).

Feature Selection

We conducted a penalized logistic regression framework via the lasso-type regularization where 0 symbolized benignity and 1 symbolized malignancy as the dependent variable. In the model, all covariates were standardized to have a mean of 0 and a standard deviation of 1. Subsequently, the model containing all parameters was fitted with a restriction: the sum of the absolute covariate coefficients must be smaller than the value t. This restriction forces some coefficients towards zero and estimates the others with shrinkage. This is an efficient approach towards obtaining a more predictive model. The size of the covariate model was determined by cross-validation, which provided a better criterion for predictive-model selection than a P value [28]. Moreover, it preserved the oracle property of variable selection [29]. Training sets were used to search for the optimal classification input features. During the searching procedure, the value of t was determined by tenfold cross-validation which gave a minimum mean cross-validated misclassification error. The fitness was better that misclassification error was smaller. The R software (R 2.13.1) and glmnet-package (Version 1.5.1; Date 2010-11-17; Authors: Jerome Friedman, Trevor Hastie, Rob Tibshirani) were implemented to select parameters.

BP Artificial Neural Network

Artificial neural networks have been successfully used as classifiers in many image analysis studies [30, 31]. The structure of the BP NN in this study contained one input layer with the number of nodes corresponding to the number of input variables (one hidden layer and one output node from 0 to 1, where 0 meant benign and 1 meant malignant). The number of hidden nodes was five nodes. The value used for convergence criteria was 0.01, and the number of iterations which assured the convergence of the network was equal to 1,000 iterations.

Validation of the Classification Methods

The area under curve (AUC) with establishing the receive operation characteristic (ROC) based on test data was used to evaluate the ability of the classifiers to differentiate benign from malignant nodules, incorporated into specificity and sensitivity according to the cutoff value of ROC curves. The malignance rate was used as the variable to draw a ROC curve. The malignance rate was defined as:

$$\text{Malignance rate} = \frac{\text{The number of malignant images of one case by prediction models}}{\text{The total number of images of one case}}$$

Also, we calculate Matthews correlation coefficient (Mcc) typically used in machine learning as a measure of the quality of binary (two-class) classifications expressed by

$$\text{Mcc} = \frac{(\text{Tp} \times \text{Tn}) - (\text{Fp} \times \text{Fn})}{(\text{Tp} + \text{Fp}) \times (\text{Tp} + \text{Fn}) \times (\text{Tn} + \text{Fp}) \times (\text{Tn} + \text{Fn})}$$

where Tp is the number of malignant nodules correctly classified as malignant and Fn is the number of benign nodules

Table 2 Results for morphological features selection

Variable	Estimate
Lobulation	2.34
Diameter	4.89
Pleural indentation	7.12
Margin	3.45
Ground-glass opacity	0.34
Nodules with an area of air	1.45
Solid	−3.44
Calcification	10.22
Maximum probability	−6.32
Sum-entropy	−10.23

wrongly classified as malignant; Tn is the number of benign nodules correctly classified as benign and Fp is the number of malignant nodules wrongly classified as benign. Mcc more closely of +1 value represents a perfect prediction, 0 an average random prediction and −1 an inverse prediction.

Results

Table 2 gave the selected features after logistic regression via lasso-type regularization. There are: lobulation, diameter of the nodule, pleural indentation, margin, ground-glass opacity, nodules with an area of air, solid, calcification, sum-entropy and maximum probability.

Utilization of the 12 radiological features alone resulted in an area under the ROC curve (AUC) of 0.84 in differentiating between malignant and benign lesions. When using selected features which combined these eight parameters with two textural features into a unified diagnostic model, the AUC was further improved to 0.91. Bootstrap was used to compare between the areas under the curve of two models (P=0.042) and the difference between two models is significant. See Fig. 2 for details. Mcc, sensitivity and specificity are listed as follows (Table 3).

Table 3 Mcc, specificity and sensitivity of models

	Mcc	Specificity	Sensitivity
Twelve radiological features	0.68	0.84	0.84
Eight radiological features and two textural features	0.78	0.80	0.96

Discussion

The management of patients with SPNs continues to be challenging. Seventy percent to 75 % of nodules that are labeled as indeterminate based on initial history and standard radiological studies may ultimately be cancerous [32]. Many validated models have been developed for computer-aided diagnosis models to differentiate malignant from benign solitary pulmonary nodules. These models were established based on factors such as clinical information (patient age, smoking status, history of cancer, and nodule size) [33, 34], morphology, and content-based image retrieval systems. Unfortunately no general breakthrough has been achieved with respect to large varied databases with documents of differing sorts and with varying characteristics. Morphological characteristics in computed tomography are however helpful in the differentiation of benign from malignant nodules because there is a kind of overlapping, and

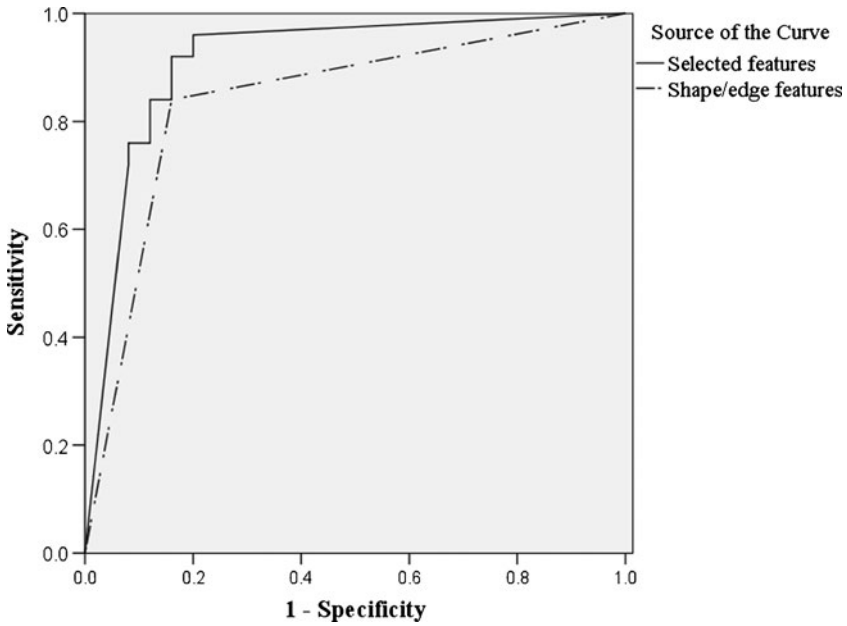

Fig. 2 ROC curve for BP NN classifiers based on six shape/edge parameters and 10 selected features

some benign nodules may show features typical of malignancy and some malignant nodules lesions may appear benign. This indicates that more advanced algorithms are needed for the diagnosis of SPN. Implementing shape/edge and textural features was done to differentiate between malignant and benign lesions on the breast MRI [35]. In the paper [18], adding textural descriptors into the morphological model was introduced for SPN.

In this study, a total of 25 subjective features which included 12 radiological and 13 textural features were extracted to gain an insight. In these radiological predictors, two important radiological features (pleural indentation and pleural effusion) were added in the prediction model for the first time.

In a medical CAD system, visual features such as shape and texture are usually included to build the system. However, using too many features in the classification algorithm can lead to over-fitting, in which noise or irrelevant features may exert undue influence on classification decisions. Lasso-type regularization to nonlinear regression model was used to select discriminative features for SPN of malignancy. The result showed that the method was extremely fast and was exploited sparsity in the input matrix where it existed. So lasso-type regularization provides an attractive regularization method for high-dimensional data in a CAD system.

When using two gray level textural features together with the eight radiological features, the AUC reached to 0.91. Our study demonstrated that the combination of radiological data and textural information in a system model is more effective. Although the image analyses are still under developing, it might be used in daily radiological practice because of its advantage. MATLAB , R, and SAS are commercially available software which were used to analyze texture features of CT image.

This is also some limitations involved in this study. All of cases in this study were obtained from hospitals, so it is difficult to balance the benign and malignant cases. Also, we did not divide the cases into obvious and subtle cases.

Acknowledgments The program of Natural Science Fund of China (Serial Number: 81172772 and 30972550); the program of Natural Science Fund of Beijing (Serial Number: 4112015); the Program of Academic Human Resources Development in Institutions of Higher Learning Under the Jurisdiction of Beijing Municipality (Serail Number: PHR201007112).

References

1. Matteis SD, Consonni D, Bertazzi PA: Exposure to occupational carcinogens and lung cancer risk. Evolution of epidemiological estimates of attributable fraction. Acta Biomed 79:34–42, 2008
2. Ries LAG, Harkins D, Krapcho M, et al: SEER Cancer Statistics Review, 1975–2003. National Cancer Institute, Bethesda, 2006
3. Winer-Muram HT: The solitary pulmonary nodule. Radiology 239 (1):34–49, 2006
4. Iwano S, Nakamura T, Kamioka Y, et al: Computer-aided differentiation of malignant from benign solitary pulmonary nodules imaged by high-resolution CT. Comput. Med. Imaging Graph 32:416–422, 2008
5. Ginneken BV, Armato III, SG, Hoop BD, et al: Comparing and combining algorithms for computer-aided detection of pulmonary nodules in computed tomography scans: the ANODE09 study. Medical Image Analysis 14:707–722, 2010
6. Way TW, Sahiner B, Chan HP, et al: Computer-aided diagnosis of pulmonary nodules on CT scans: improvement of classification performance with nodule surface features. Medical Physics 36 (7):3086–3098, 2008
7. Yeh C, Lin CL, Wu MT, et al: A neural network-based diagnostic method for solitary pulmonary nodules. Neurocomputing 72:612–624, 2008
8. McCarville MB, Lederman HM, Santana VM, et al: Distinguishing benign from malignant pulmonary nodules with helical chest CT in children with malignant solid tumors. Radiology 239(2):514–520, 2006
9. Avci E, Sengur A, Hanbay D: An optimum feature extraction method for texture classification. Expert Syst Appl 36:6036–6043, 2009
10. Müller H, Michoux N, Bandon D, et al: A review of content-based image retrieval systems in medical applications—clinical benefits and future directions. International Journal of Medical Informatics 73:1–23, 2004
11. Ondimu S, Murase NH: Effect of probability-distance based Markovian texture extraction on discrimination in biological imaging. Comput Electron Agric 63(1):2–12, 2008
12. Dettori L, Semler L: A comparison of wavelet, ridgelet, and curvelet-based texture classification algorithms in computed tomography. Computers in Biology and Medicine 37:486–498, 2009
13. Erasmus JJ, Connolly JE, McAdams HP, et al: Solitary pulmonary nodules: part I. Morphologic evaluation for differentiation of benign and malignant lesions. Radiographics 20(1):43–58, 2000
14. Erasmus JJ, McAdams HP, Connolly JE: Solitary pulmonary nodules: part II. Evaluation of the indeterminate nodule. Radiographics 20(1):59–66, 2000
15. Nakamura K, Yoshida H, Engelmann R, et al: Computerized analysis of the likelihood of malignancy in solitary pulmonary nodules with use of artificial neural networks. Radiology 214:823–830, 2000
16. Li F, Shusuke S, Hiroyuki A, et al: Malignant versus benign nodules at CT screening for lung cancer: comparison of thin-section ct findings. Radiology 233:793–798, 2004
17. Wang H, Guo XH, Jia ZW, et al: Multilevel binomial logistic prediction model for malignant pulmonary nodules based on texture features of CT image. Eur J Radiol 74:124–129, 2010
18. Lee MC, Boroczky L, Sungur-Stasik K, et al: Computer-aided diagnosis of pulmonary nodules using a two-step approach for feature selection and classifier ensemble construction. Artificial Intelligence in Medicine 50:43–53, 2010
19. Zhu YJ, Tan YQ, Hua YQ, et al: Feature selection and performance evaluation of support vector machine (svm)-based classifier for differentiating benign and malignant pulmonary nodules by computed tomography. Journal of Digital Imaging 23(1):51–65, 2010
20. Li Y, Chen KZ, Wang J: Development and validation of a clinical prediction model to estimate the probability of malignancy in solitary pulmonary nodules in Chinese people. Clinical Lung Cancer 12(5):313–319, 2011

21. Zhang Y, Jin J, Qing XY, et al: LASSO based stimulus frequency recognition model for SSVEP BCIs. Biomedical Signal Processing and Control 7(2):104–111, 2011
22. Han SD, Tao WB, Wu XL: Texture segmentation using independent-scale component-wise Riemannian-covariance Gaussian mixture model in KL measure based multi-scale nonlinear structure tensor space. Pattern Recognition 44(3):503–518, 2011
23. Zhang M, Zhu J, Djurdjanovic D, Ni J: A comparative study on the classification of engineering surfaces with dimension reduction and coefficient shrinkage methods. J Manuf Syst 25(3):209–220, 2007
24. Arora S, Acharya J, Verma A, et al: Multilevel thresholding for image segmentation through a fast statistical recursive algorithm. Pattern Recognit Lett 29:119–125, 2008
25. Taheri S, Ong SH, Chong VFH: Level-set segmentation of brain tumors using a threshold-based speed function. Image and Vision Computing 28:26–37, 2010
26. Haralick RM, Shanmugam K, Dinstein I: Textural features for image classification. IEEE Trans Syst Man Cybernet 3:610–621, 1973
27. Haralick RM: Statistical and structural approaches to texture. Proc IEEE 67(5):786–804, 1979
28. Ribbing J, Nyberg J, Caster O, Jonsson EN: The lasso—a novel method for predictive covariate model building in nonlinear mixed effects models. J Pharmacokinet Pharmacodyn 34:485–517, 2007
29. Zou H: The adaptive lasso and its oracle properties. J Am Stat Assoc 101:1418–1429, 2006
30. Newell D, Nie K, Chen JH, et al: Selection of diagnostic features on breast MRI to differentiate between malignant and benign lesions using computer-aided diagnosis: differences in lesions presenting as mass and non-mass-like enhancement. Eur Radiol 20:771–781, 2010
31. Markopoulos C, Kouskos E, Koufopoulos K: Use of artificial neural networks (computer analysis) in the diagnosis of micro-calcifications on mammography. Eur J Radiol 39:60–65, 2001
32. Behzadi A, Ung Y, Lowe V, et al: The role of positron emission tomography in the management of non–small cell lung cancer. Can J Surg 52(3):235–242, 2009
33. Gould MK, Ananth L, Barnett PG: A clinical model to estimate the pretest probability of lung cancer in patients with solitary pulmonary nodules. Chest 131(2):383–388, 2007
34. Herder GJ, Tinteren HV, Golding RP, et al: Clinical prediction model to characterize pulmonary nodules. Chest 128:2490–2496, 2005
35. Newell D, Nie K, Chen JH: Selection of diagnostic features on breast MRI to differentiate between malignant and benign lesions using computer-aided diagnosis: differences in lesions presenting as mass and non-mass-like enhancement. Eur Radiol 20:771–781, 2010